

Electronic Supplementary Information (ESI) for

# A General and Selective Ni-Catalysed Reductive Amination using Hydrazine Hydrate as Facile Nitrogen and Hydrogen Sources

Jiazheng Zhu,<sup>‡a</sup> Chengjie Duan,<sup>‡a</sup> Sen Ye,<sup>d</sup> Qizhong Zhang,<sup>c</sup> Kun Li,<sup>a</sup> Guangke He,<sup>a</sup> Xiang Liu,<sup>\*,a,c</sup> and Zhiguo Zhang<sup>\*,b,c</sup>

a. School of Chemistry and Molecular Engineering, Nanjing Tech University, Nanjing 211816, China.

b. Key Laboratory of Biomass Chemical Engineering of Ministry of Education, College of Chemical and Biological Engineering, Zhejiang University, 38 Zheda Road, Hangzhou 310027, China.

c. Institute of Zhejiang University-Quzhou, Quzhou 32400, China

d. Morningside Laboratory for Chemical Biology and Department of Chemistry, The University of Hong Kong, Pokfulam Road, Hong Kong, China

e. Anhui Haihua Chemical Technology Group Co.,Ltd., Bengbu 233000, China

‡ These authors contributed equally to this work.

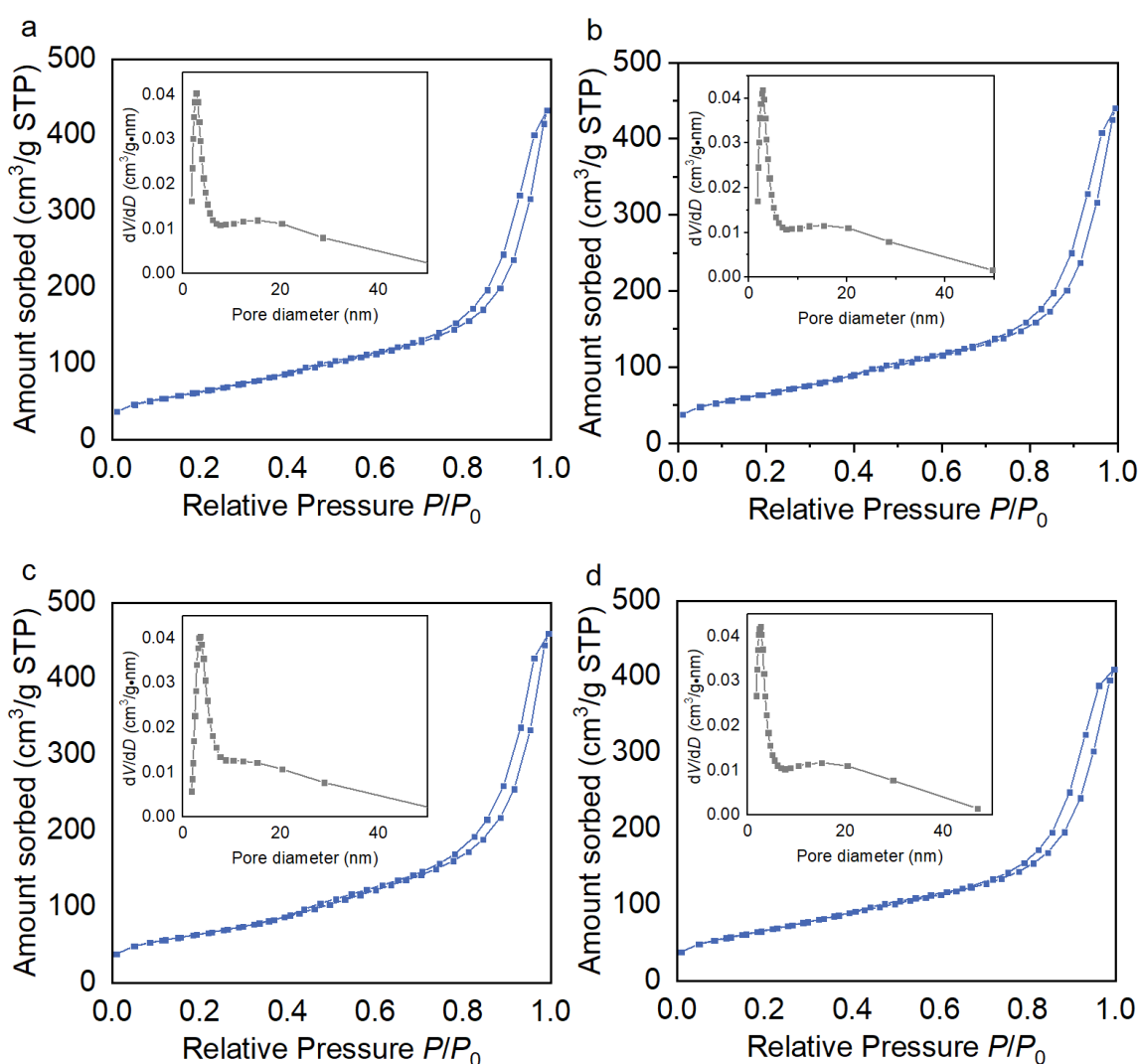


**Figure S1.** N<sub>2</sub> adsorption-desorption isotherms and the BJH pore size distribution (inset) of (a) Ni/meso-Al<sub>2</sub>O<sub>3</sub>-400; (b) Ni/meso-Al<sub>2</sub>O<sub>3</sub>-500; (c) Ni/meso-Al<sub>2</sub>O<sub>3</sub>-600; (d) Ni/meso-Al<sub>2</sub>O<sub>3</sub>-700.

**Table S1.** Physicochemical properties for various Ni/*meso*-Al<sub>2</sub>O<sub>3</sub>-*T* catalysts.

Entry	Catalyst	$S_{\text{BET}}$ ( $\text{m}^2 \cdot \text{g}^{-1}$ ) <sup>a</sup>	$V_{\text{p}}$ ( $\text{cm}^3 \cdot \text{g}^{-1}$ ) <sup>a</sup>	$D_{\text{p}}$ (nm) <sup>a</sup>	Actual Ni loading (wt%) <sup>b</sup>
1	Ni/ <i>meso</i> -Al <sub>2</sub> O <sub>3</sub> -400	234	0.669	11	6.50
2	Ni/ <i>meso</i> -Al <sub>2</sub> O <sub>3</sub> -500	240	0.679	11	6.60
3	Ni/ <i>meso</i> -Al <sub>2</sub> O <sub>3</sub> -600	231	0.686	11	6.62
4	Ni/ <i>meso</i> -Al <sub>2</sub> O <sub>3</sub> -700	246	0.607	10	6.79

<sup>a</sup> Specific surface area ( $S_{\text{BET}}$ ), cumulative pore volume ( $V_{\text{p}}$ ), and pore diameter ( $D_{\text{p}}$ ) were determined by N<sub>2</sub> physisorption. <sup>b</sup> Actual Ni loadings were determined by ICP-OES.

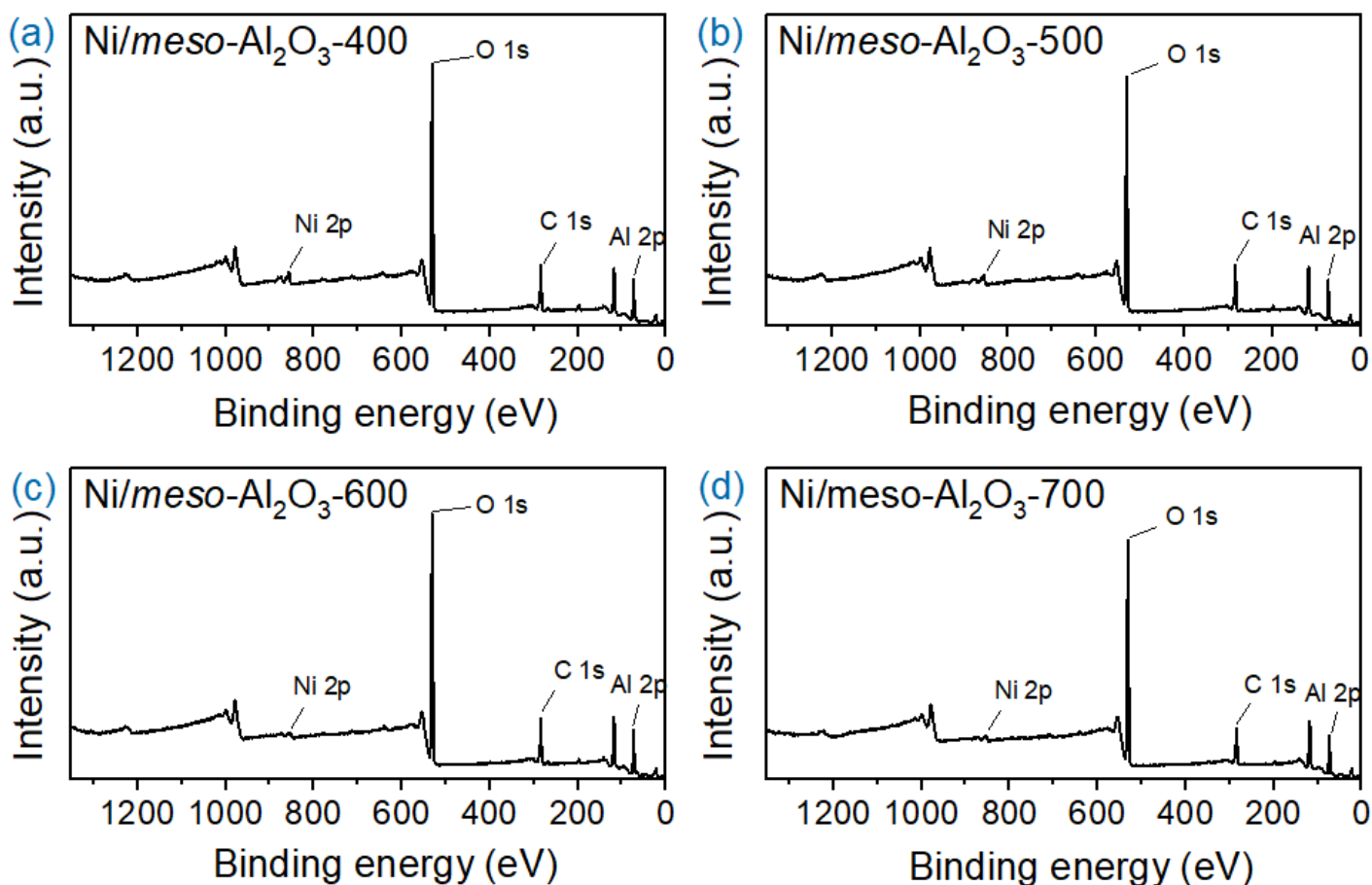


**Figure S2.** Full-scan XPS spectrum of (a) Ni/*meso*-Al<sub>2</sub>O<sub>3</sub>-400; (b) Ni/*meso*-Al<sub>2</sub>O<sub>3</sub>-500; (c) Ni/*meso*-Al<sub>2</sub>O<sub>3</sub>-600; (d) Ni/*meso*-Al<sub>2</sub>O<sub>3</sub>-700.

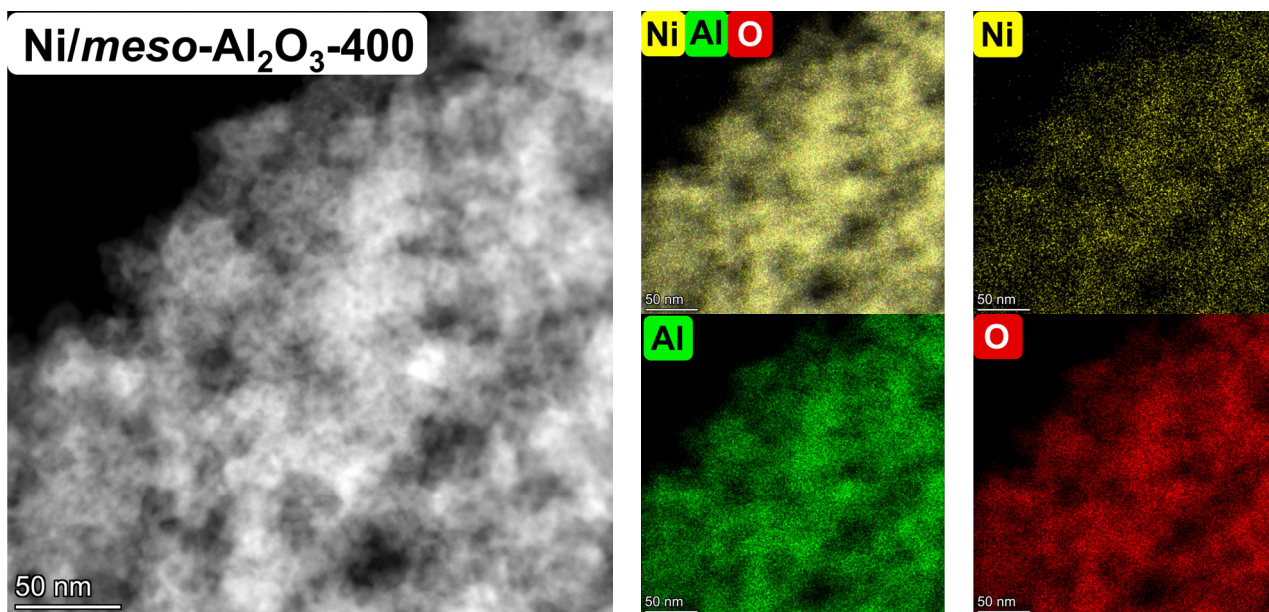


**Figure S3.** HAADF-STEM image and representative EDS elemental maps of nickel (yellow), alumina (green), and oxygen (red) for Ni/meso-Al<sub>2</sub>O<sub>3</sub>-400.

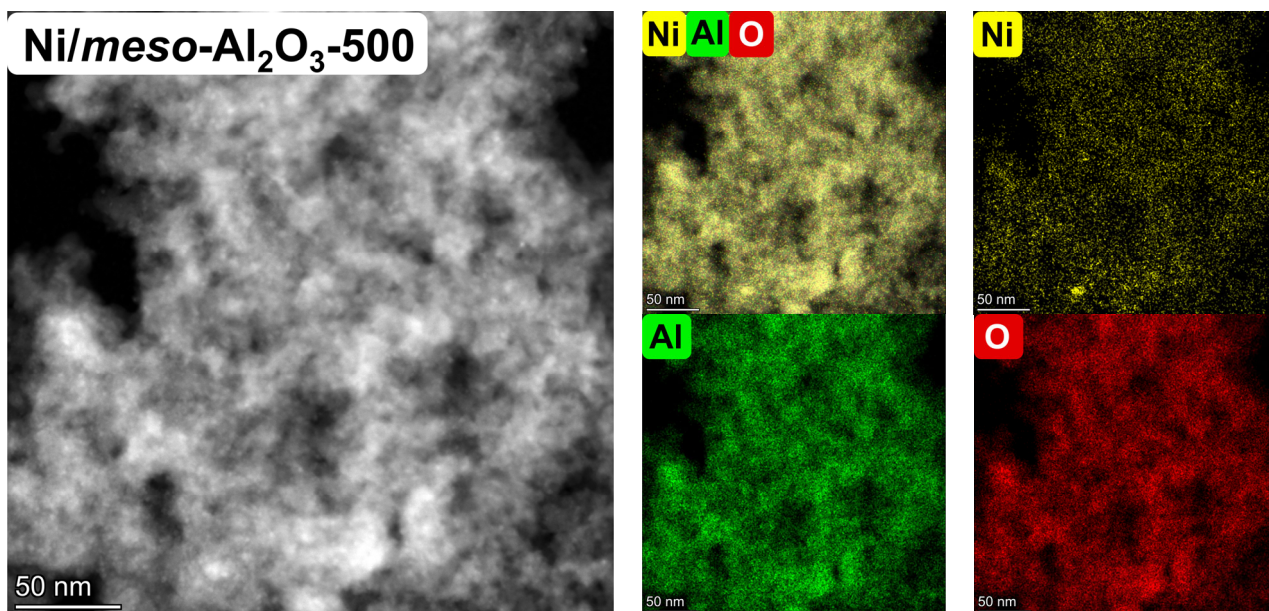


**Figure S4.** HAADF-STEM image and representative EDS elemental maps of nickel (yellow), alumina (green), and oxygen (red) for Ni/meso-Al<sub>2</sub>O<sub>3</sub>-500.



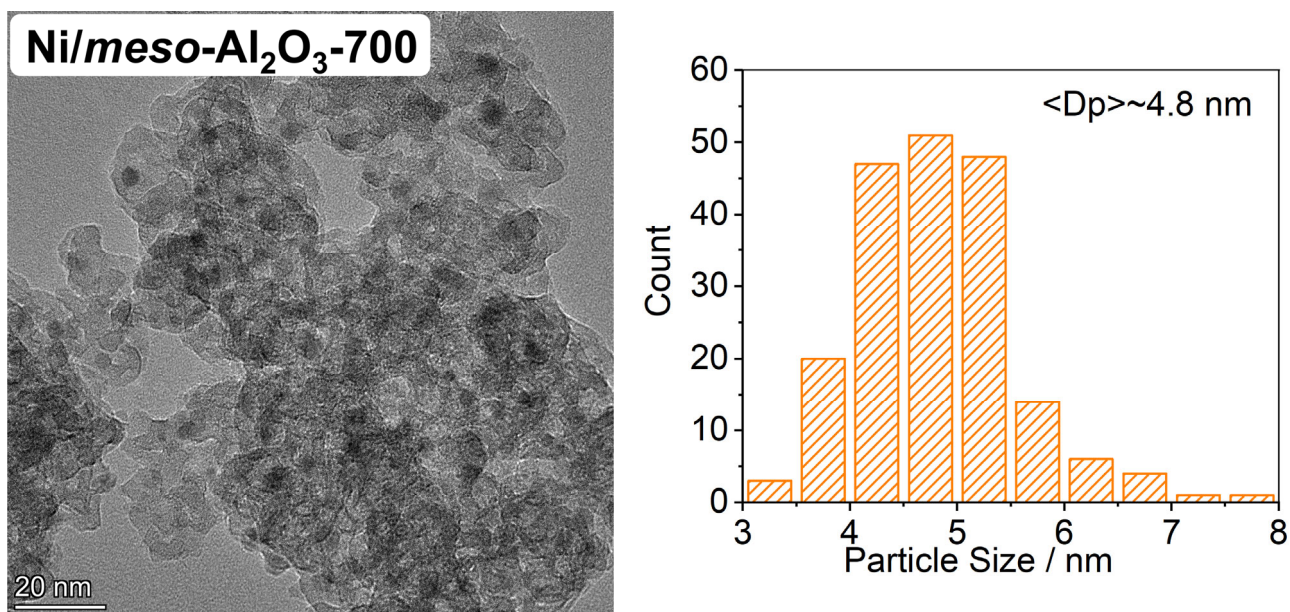


**Figure S5.** TEM image and Ni particle size distribution of Ni/meso-Al<sub>2</sub>O<sub>3</sub>-700.

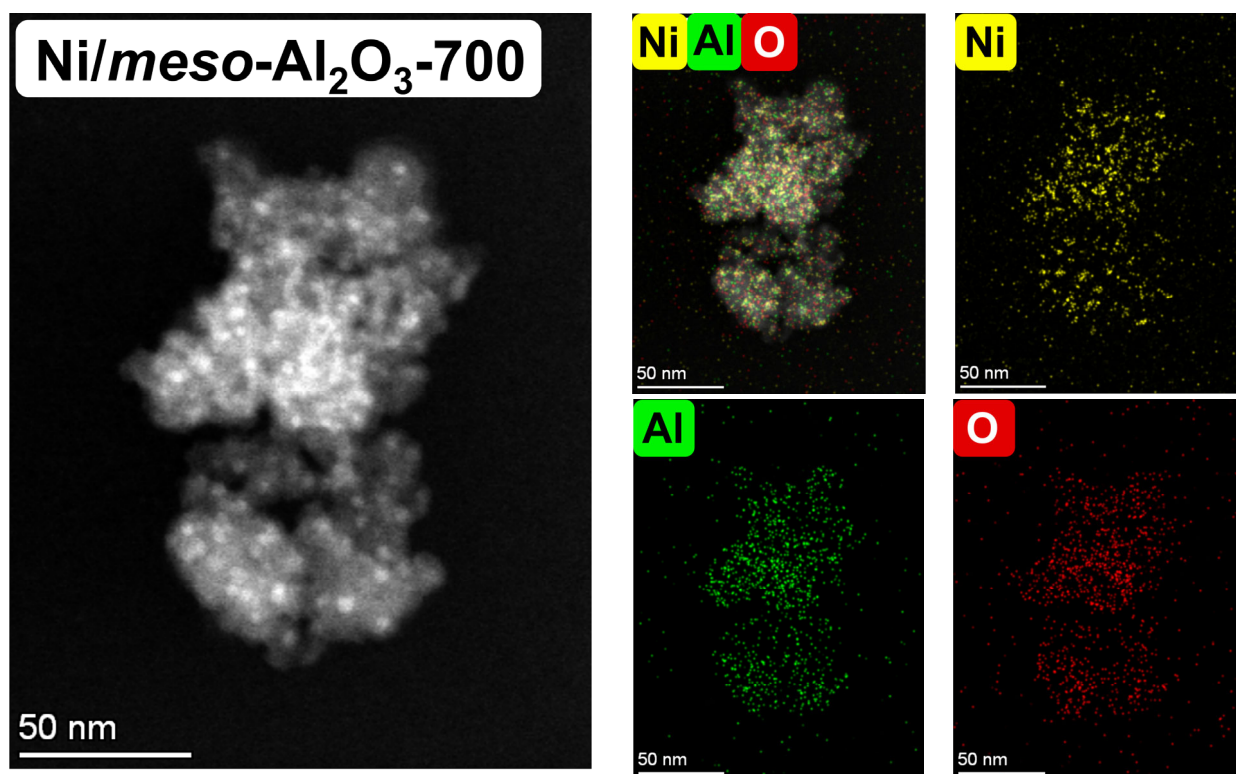
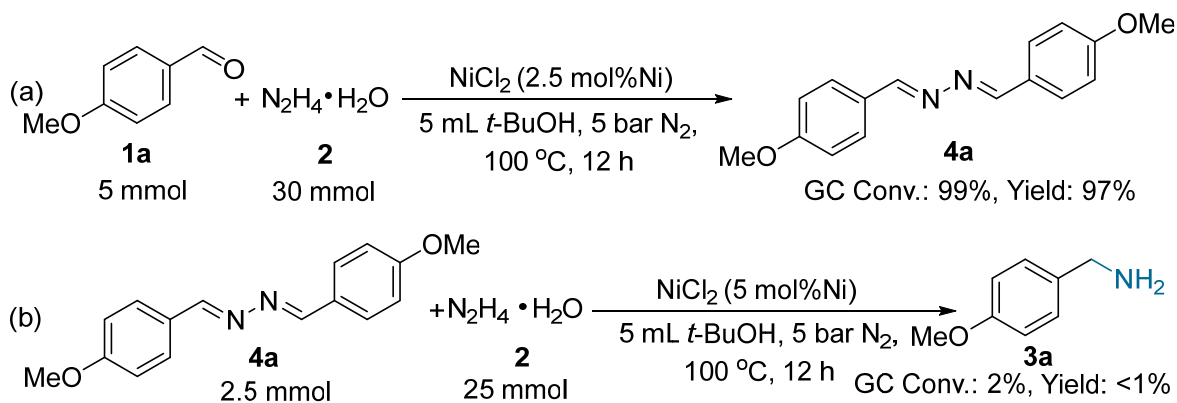


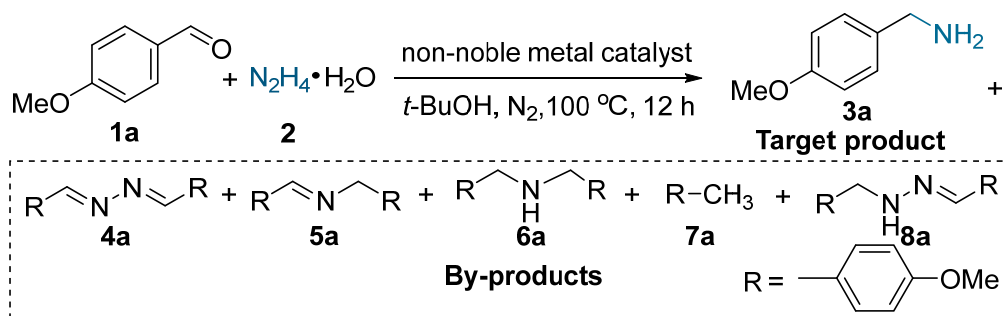
**Figure S6.** HAADF-STEM image and representative EDS elemental maps of nickel (yellow), alumina (green), and oxygen (red) for Ni/meso-Al<sub>2</sub>O<sub>3</sub>-700.





**Scheme S1.** Control experiments for the reactions of **1a** and **4a** in the presence of NiCl<sub>2</sub>.

**Table S2.** Reductive amination of 4-methoxybenzyl aldehyde (**1a**) with hydrazine hydrate (**2**) over different catalysts.<sup>a</sup>



Entry	Catalyst	Conv. (%)	Yield (%) <sup>b</sup>					
			3a	4a	5a	6a	7a	8a
1	Ni/MgO-600	100	70	0	8	11	11	0
2	Ni/ZnO-600	100	51	10	0	39	0	0
3	Ni/CeO <sub>2</sub> -600	100	17	83	0	0	0	0
4	Ni/Nb <sub>2</sub> O <sub>5</sub> -600	100	16	82	0	0	0	0
5	Fe/ <i>meso</i> -Al <sub>2</sub> O <sub>3</sub> -600	100	0	93	1	0	0	6
6	Co/ <i>meso</i> -Al <sub>2</sub> O <sub>3</sub> -600	100	0	98	0	0	0	1
7	Cu/ <i>meso</i> -Al <sub>2</sub> O <sub>3</sub> -600	100	0	95	0	0	0	4

<sup>a</sup>Reaction conditions: 4-methoxy benzaldehyde (5.0 mmol), hydrazine hydrate (30 mmol), catalyst (2.5 mol% metal based on **1a**), *t*-BuOH (5.0 mL), 100 °C, 5 bar N<sub>2</sub>, 12 h; n.r.=no reaction. <sup>b</sup>Conversions and yields were determined by GC-MS and GC analysis based on the consumption of **1a**.

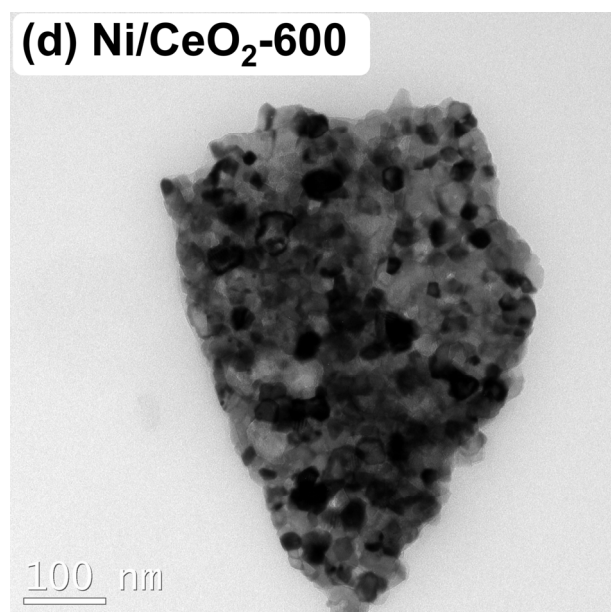
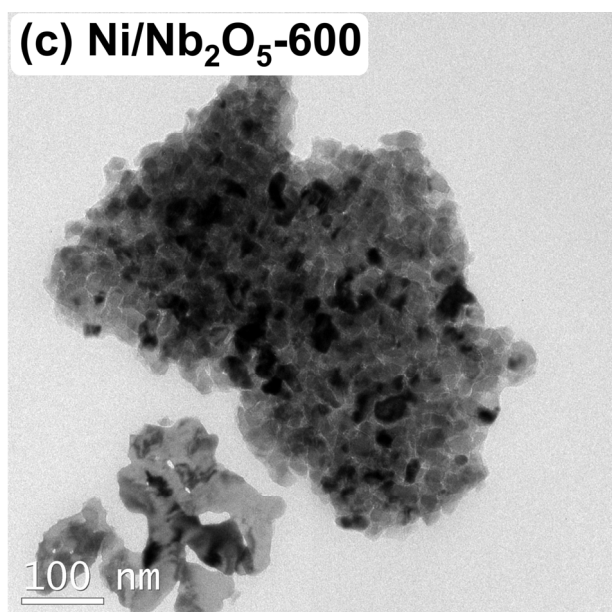
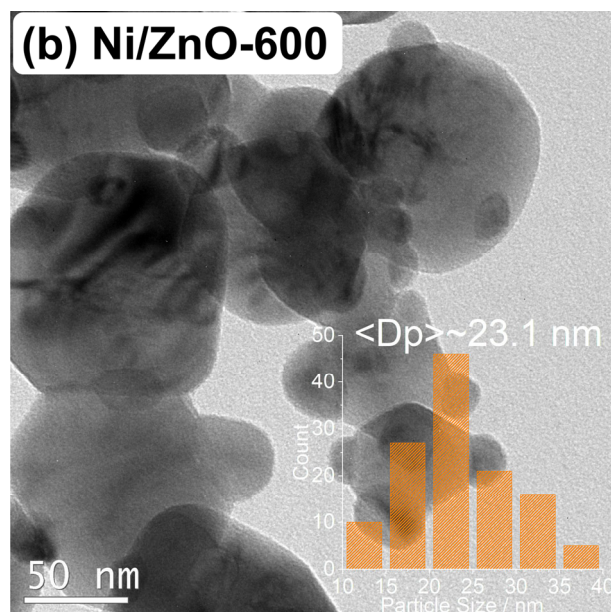
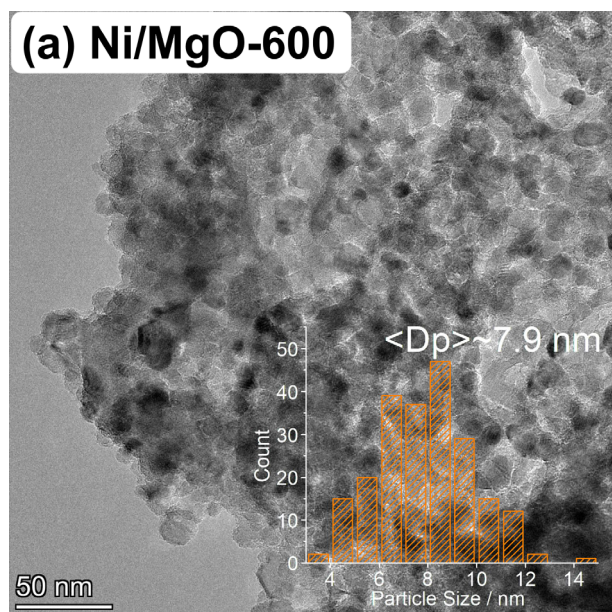


**Figure S7.** TEM image and Ni particle size distribution of (a) Ni/MgO-600, (b) Ni/ZnO-600, (c) Ni/Nb<sub>2</sub>O<sub>5</sub>-600, (d) Ni/CeO<sub>2</sub>-600.

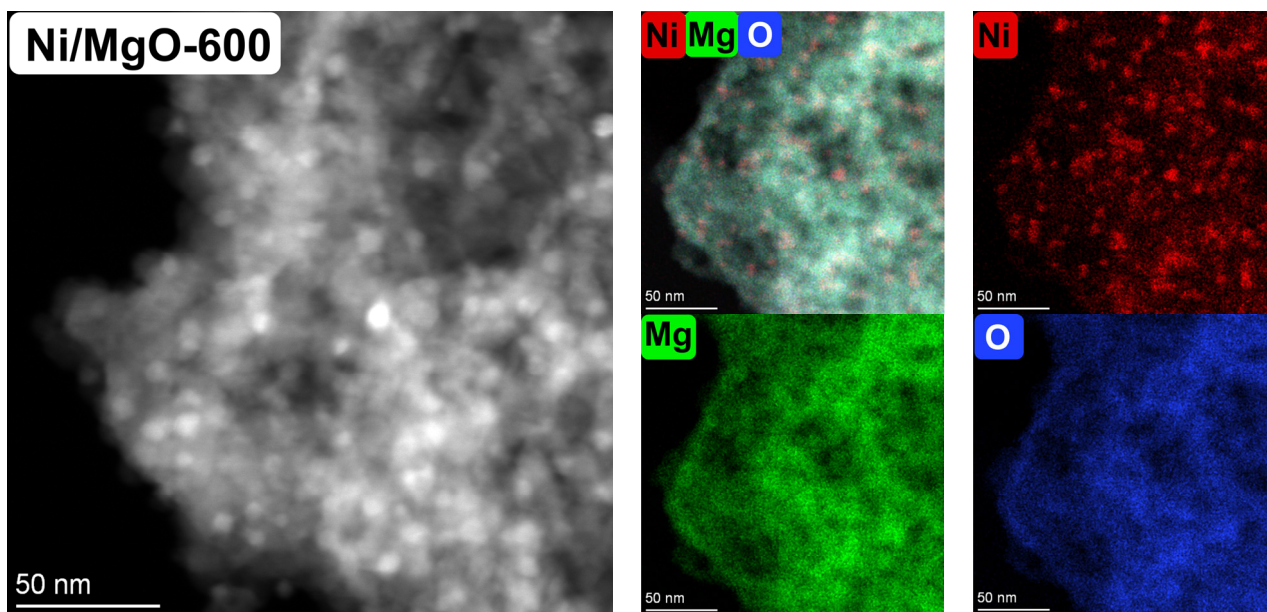


**Figure S8.** HAADF-STEM image and representative EDS elemental maps of nickel (red), magnesium (green), and oxygen (blue) for Ni/MgO-600.

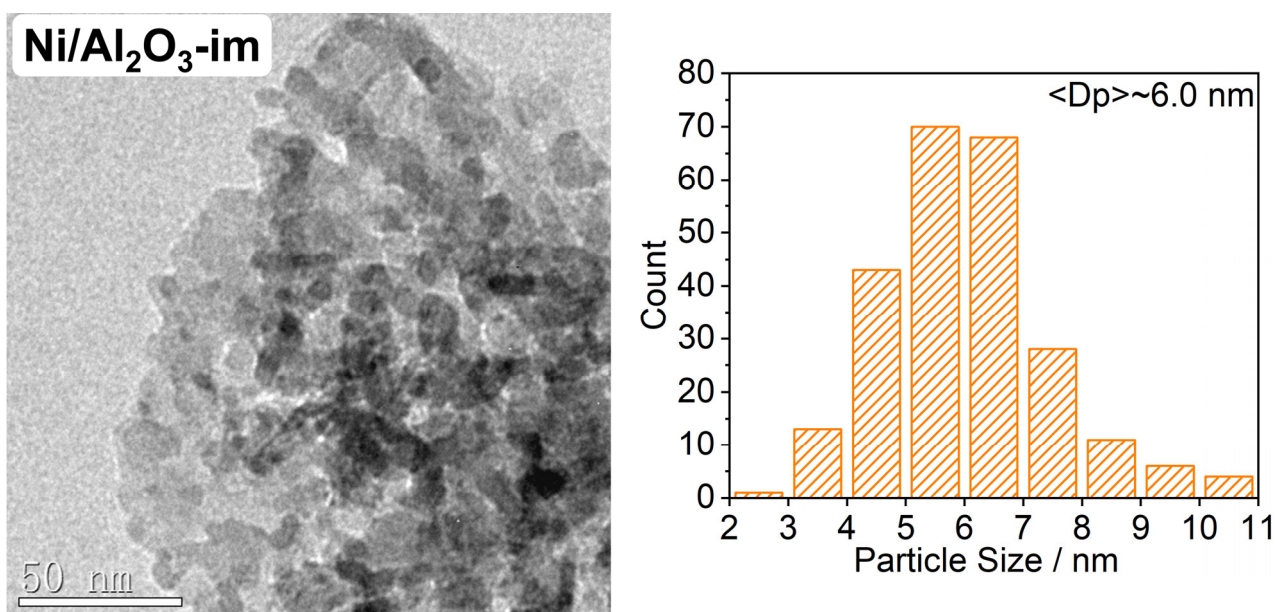
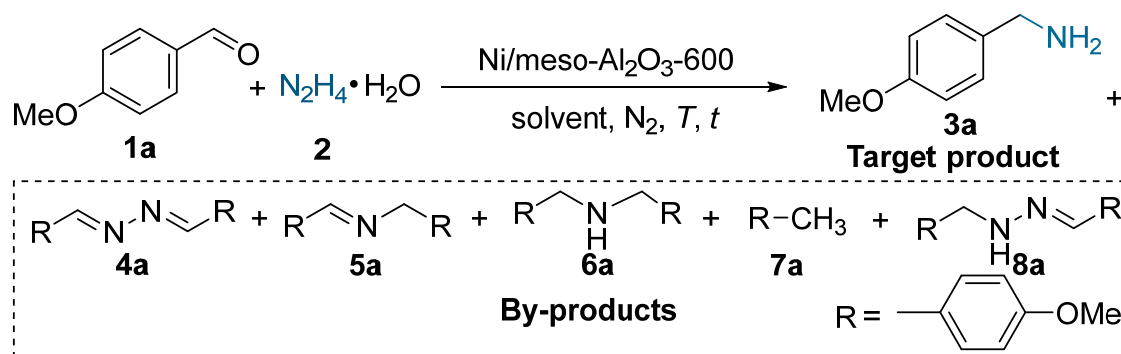


**Figure S9.** TEM image and Ni particle size distribution of Ni/Al<sub>2</sub>O<sub>3</sub>-im.



**Table S3.** Ni/*meso*-Al<sub>2</sub>O<sub>3</sub>-600 catalyzed reduction of 4-methoxy benzaldehyde (**1a**) and N<sub>2</sub>H<sub>4</sub>·H<sub>2</sub>O (**2**) under different reaction conditions <sup>a</sup>



Entry	Solvent	Ni mol% <sup>b</sup>	N <sub>2</sub> (bar)	N <sub>2</sub> H <sub>4</sub> (mmol)	solvent volume (mL)	T (°C)	Conv. (%) <sup>c</sup>	Yield (%) <sup>c</sup>						
								<b>3a</b>	<b>4a</b>	<b>5a</b>	<b>6a</b>	<b>7a</b>	<b>8a</b>	<b>others</b>
1	<i>t</i> -BuOH	2.5	5	30	5	100	100	<b>92</b>	0	3	0	5	0	0
2	MeOH	2.5	5	30	5	100	100	<b>69</b>	4	0	16	7	4	0
3	THF	2.5	5	30	5	100	100	<b>65</b>	19	2	0	2	0	12
4	toluene	2.5	5	30	5	100	100	<b>51</b>	13	24	2	5	0	5
5	<i>n</i> -hexane	2.5	5	30	5	100	100	<b>47</b>	4	0	44	5	0	0
6	<i>t</i> -BuOH	2.5	5	30	3	100	100	<b>87</b>	2	4	2	5	0	0
7	<i>t</i> -BuOH	2.5	5	30	4	100	100	<b>86</b>	9	0	0	3	0	2
8	<i>t</i> -BuOH	2.5	5	30	6	100	100	<b>78</b>	17	0	0	2	0	3
9	<i>t</i> -BuOH	2.5	5	30	7	100	100	<b>75</b>	20	0	0	3	0	2
10	<i>t</i> -BuOH	2.5	5	10	5	100	100	<b>12</b>	15	0	47	7	14	5
11	<i>t</i> -BuOH	2.5	5	20	5	100	100	<b>57</b>	6	0	30	4	3	0
12	<i>t</i> -BuOH	2.5	5	25	5	100	100	<b>75</b>	17	0	4	2	0	2
13	<i>t</i> -BuOH	2.5	5	35	5	100	100	<b>91</b>	2	0	4	4	0	0
14	<i>t</i> -BuOH	2.5	5	40	5	100	100	<b>91</b>	5	0	4	4	0	0
15	<i>t</i> -BuOH	2.5	5	30	5	90	100	<b>77</b>	13	4	2	0	4	0
16	<i>t</i> -BuOH	2.5	5	30	5	110	100	<b>81</b>	1	2	2	13	1	0
17	<i>t</i> -BuOH	1.2	5	30	5	100	100	<b>81</b>	15	0	0	2	0	2
18	<i>t</i> -BuOH	5	5	30	5	100	100	<b>81</b>	0	3	0	11	0	5
19	<i>t</i> -BuOH	5	1	30	5	100	100	<b>86</b>	8	0	1	3	0	2
20	<i>t</i> -BuOH	5	10	30	5	100	100	<b>74</b>	6	5	0	6	0	6

<sup>a</sup> Reaction conditions: 4-methoxy benzaldehyde (5.0 mmol), hydrazine hydrate, Ni/*meso*-Al<sub>2</sub>O<sub>3</sub>-600, N<sub>2</sub>, 12 h. <sup>b</sup> Based on **1a**. <sup>c</sup> Conversions and yields were determined by GC-MS and GC analysis based on the consumption of **1a**.

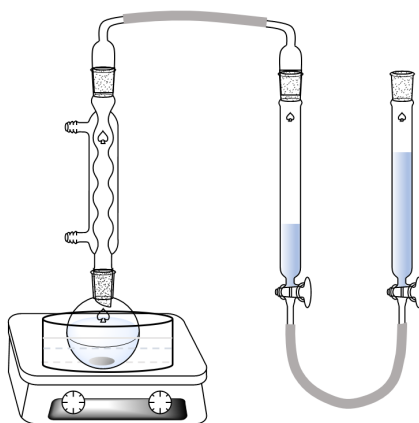
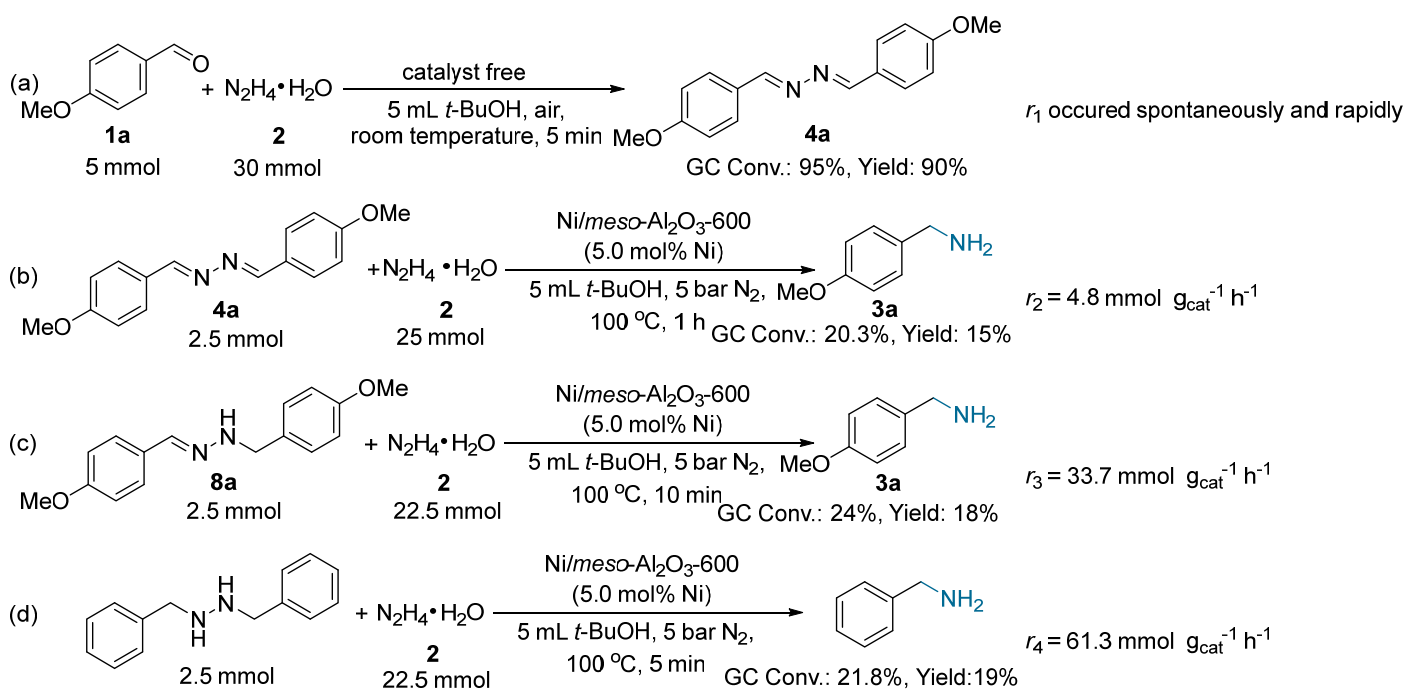
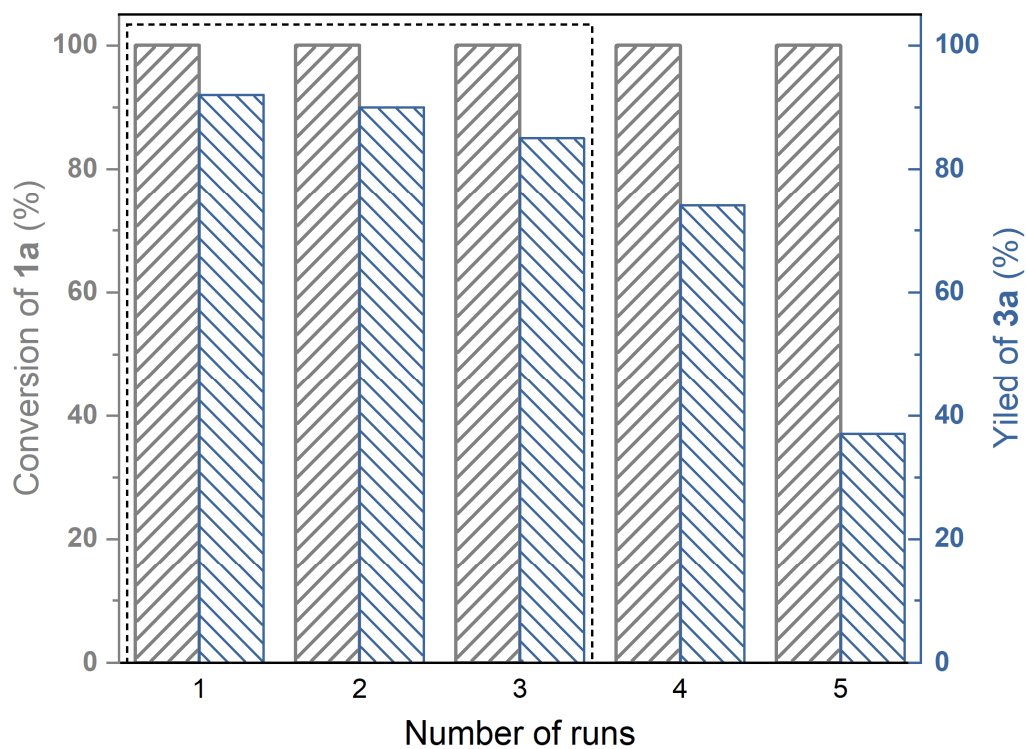


**Figure S10.** The equipment for hydrazine decomposition reaction. The reaction was initiated by adding 30 mmol hydrazine hydrate into a round bottom flask containing *t*-BuOH (5 mL) and Ni/*meso*-Al<sub>2</sub>O<sub>3</sub>-600 (106.7 mg). The reaction temperature (100 °C) was controlled by oil bath. The volume change of H<sub>2</sub> and N<sub>2</sub> was detected by a gas barrette and used for the calculation of N<sub>2</sub>H<sub>4</sub> conversion. After 12 hrs reaction, 1180 mL gas was produced (calculated at room temperature, ~25 °C). The conversion of hydrazine was calculated by assuming the all the consumed N<sub>2</sub>H<sub>4</sub> was converted into H<sub>2</sub> and N<sub>2</sub>:

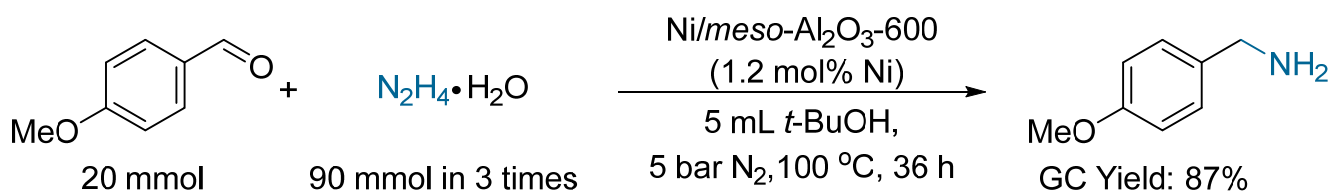
$$\text{Conv. \%} = \left[ \frac{pV}{R(t/^{\circ}\text{C} + 273.15)} \times \frac{1}{3} \right] / n_{\text{N}_2\text{H}_4}$$



**Scheme S2.** Initial reaction rate for steps involved in the N<sub>2</sub>H<sub>4</sub>-involved reductive amination.



**Figure S11.** Recycle experiments using Ni/*meso*-Al<sub>2</sub>O<sub>3</sub>-600 catalyst in the reaction of 4-methoxy benzaldehyde with hydrazine hydrate.



**Scheme S3.** Gram-scale reductive amination of 4-methoxybenzyl aldehyde with N<sub>2</sub>H<sub>4</sub>·H<sub>2</sub>O.